The International Society of Precision Agriculture presents the
15th International Conference on Precision Agriculture
26–29 JUNE 2022
Minneapolis Marriott City Center | Minneapolis, Minnesota USA

Deep Learning-Based Corn Disease Tracking Using RTK Geolocated UAS Imagery

Aanis Ahmad[1], Varun Aggarwal[1], *Dharmendra Saraswat[2], Aly El Gamal[1], and Guri Johal[3]

[1] Elmore Family School of Electrical and Computer Engineering, Purdue University, West Lafayette, IN, US.
[2] Department of Agricultural and Biological Engineering, Purdue University, West Lafayette, IN, US.
[3] Department of Botany and Plant Pathology Engineering, Purdue University, West Lafayette, IN, US.

*Corresponding Author: saraswat@purdue.edu

A paper from the Proceedings of the
15th International Conference on Precision Agriculture
June 26-29, 2022
Minneapolis, Minnesota, United States

Abstract.

Deep learning-based solutions for precision agriculture have achieved promising results in recent times. Deep learning has been used to accurately classify different disease types and disease severity estimation as an initial stage for developing robust disease management systems. However, tracking the spread of diseases, identifying disease hot spots within cornfields, and notifying farmers using deep learning and UAS imagery remains a critical research gap. Therefore, in this study, high resolution, Unmanned Aerial System (UAS) acquired, Real-Time Kinematic (RTK) geotagged, RGB imagery at heights of 3 meters and 12 meters above ground level (AGL), was used to track disease hot spots in corn fields throughout the growing season. A total of 98,000 RGB images with a resolution of 8192 x 5460 pixels were acquired in cornfields located at Purdue University's Agronomy Center for Research and Education (ACRE), using a DJI Matrice 300 with an RTK base station mounted with a 45-megapixel DJI Zenmuse P1 camera, from June 28th to August 31st, 2021. After carefully selecting images acquired at one-week intervals, they were split into multiple smaller tiles and superpixels using the Simple Linear Iterative Clustering (SLIC) segmentation algorithm. Images were first split into tiles of sizes 250 x 250 pixels, 500 x 500 pixels, and 1000 x 1000 pixels, resulting in 672, 160, and 40 image tiles, respectively. Additionally, for SLIC segmentation, the images were split into the same number of superpixels as the number of tiles using two different compactness (m) values. After the tiles and superpixels were created, they were labeled as either soil, weed, healthy corn, or diseased corn.

Five Convolutional Neural Network (CNN) architectures, namely VGG16, ResNet50, InceptionV4, DenseNet169, and Xception, were then used to train deep learning-based image classification models to compare the tile-based approach and SLIC segmentation for disease tracking in cornfields. After comparing the trained deep learning models using testing accuracies and testing losses, the optimal number of tiles and SLIC segmented superpixels were identified with the help of a plant pathologist. It was observed that the DenseNet169 model that was used to identifying the diseased regions when images were segmented into tiles of sizes 1000 x 1000 pixels achieved performed the best with testing accuracy of 100% and testing loss of 0.0007. The best performing model was then used to calculate the percentage of each diseased image by highlighting diseased regions. In addition, the RTK geolocation information for each image was used to update farmers with the location of disease hot spots within cornfields by developing a web and smartphone application and sending email message notifications.

Keywords.
Deep learning, Disease Identification, SLIC Segmentation, Image Classification, UAS, Web Application, Smartphone Application.

Introduction

As diseases pose a serious threat to crop production systems worldwide (Chen et al., 2021), research is underway to develop high-throughput precision agricultural solutions for disease management in fields. Most current solutions rely on pesticide application over entire fields, which is destructive to healthy crops and incurs high economical costs (Tudi et al., 2021). Furthermore, these ineffective approaches are subjective (Bock et al., 2010). Therefore, there is a need for the development of effective solutions capable of identifying the different diseased regions which will essentially help overcome the limitations presented by approaches that are widely practiced.

Recently, researchers have relied on deep learning-based computer vision for developing solutions for various precision agricultural solutions including weed identification (Ahmad et al., 2021a), disease identification (Ahmad et al., 2021b), disease severity estimation (Wang et al., 2019), insect identification (Thenmozhi et al., 2019), insect counting (Tetila et al., 2019), crop counting (Kitano et al., 2019), crop height estimation (Xie et al., 2021), yield prediction (Wang et al., 2018), etc. In addition, different sensors have been used for acquiring imagery for training robust deep learning models, including UAS (Etienne et al., 2021), handheld (Jahan et al., 2021), mounts (Wiesner-Hanks et al., 2018), and ground robot platforms (Young et al., 2019).

In particular, deep learning has been used extensively for crop disease diagnosis within the past seven years. Deep learning was used for identification of diseases in crops using UAS imagery acquired using hyperspectral sensors (Zhu et al., 2017; Nguyen et al., 2021). Multispectral imagery was also used for plant disease identification (Kerkech et al., 2020). Although spectral sensors are capable of accurately locating diseased regions, they are costly and difficult to operate (Farber et al., 2019). RGB sensors on the other cost less and are easy to operate (Ngugi et al., 2021). Therefore, the use of RGB sensors has gained popularity. Deep learning was recently used for accurate disease identification using UAS imagery acquired by utilizing RGB sensors (Wu et al., 2019).

Although current studies have shown promising results, in order to develop an effective disease management system, the diseased regions present within fields need to be accurately identified with their location for farmers to accurately navigate to hot spot regions within the field. Recently, a deep learning-based approach was developed using a sliding window approach to accurately identify the diseased regions in corn fields with testing accuracies of up to 97.84% (Ahmad et al., 2021b). However, additional segmentation approaches were not explored and the GPS information from the UAS imagery was not harnessed to develop an application to alert farmers of existing diseased hot spots within corn fields.

Multiple different computer vision segmentation approaches have been proposed over the years. Recently, simple linear iterative clustering (SLIC) segmentation approach was proposed (Achanta, 2010). SLIC segmentation is a promising, fast, and computationally efficient method

that can be used to create superpixels corresponding to similar regions within an image (Achanta et al., 2012). SLIC segmentation was recently used for precision agricultural applications such as insect counting (Tetila et al., 2019a), tree detection in urban area (Martins et al., 2021), and plant disease identification (Tetila et al., 2019b; Trindade et al., 2020).

In this study, deep learning was used to train disease regions identification models using tile segmented images and superpixels created using SLIC segmentation. A total of 25 deep learning models were trained using state-of-the-art deep neural network architectures: namely VGG16, ResNet50, InceptionV3, DenseNet169, and Xception. After comparing the different techniques for splitting the images, the RTK geolocation information for each image that was uploaded was obtained. The farmer was then notified of diseased regions in corn fields using RTK geolocation and the deep learning model to indicate the percentage of the field infected at the location at which the image was acquired. Five primary objectives were identified for developing a disease regions hot spot location tool to help farms manage diseases:

1. Acquire a large UAS imagery dataset.
2. Use tile segmentation on UAS imagery to create datasets with tiles of sizes 250 x 250, 500 x 500, and 1000 x 1000 pixels.
3. Use SLIC Segmentation to create superpixels using two different K values of 5 and 10.
4. Train deep learning models to compare the different segmentation approaches for disease region identification.
5. Develop an application for alerting farmers of diseased hot spots in corn fields using RTK geolocated images.

Materials and Methods

Dataset

For the purpose of this study, a custom dataset consisting of a total of 98,000 RGB images that were acquired using a DJI Matrice 300 UAS with an RTK base station was used. The UAS was mounted with a Zenmuse P1 45 Megapixel camera capable of acquiring images with a resolution of 8192 x 5460 pixels. The images were acquired by conducting multiple flights at five, 12, and 20 meters, over corn field 21B located at Purdue University's Agronomy Center of Research (ACRE) from June 13th to August 31st, 2021.

Tile Based Segmentation

After obtaining the images, a total of 500 images were randomly selected from different dates and heights for the purpose of this study. The images were then subject to splitting into tiles of various sizes, i.e., 1000 x 1000, 500 x 500, and 250 x 250 pixels, in order to prepare datasets for training deep learning models capable of accurately identifying different diseased regions in corn fields. After an original image of size 8192 x 5460 pixels was split, a total of 672, 160, and 40 images were obtained for 250 x 250, 500 x 500, and 1000 x 1000 pixels, respectively as shown in figure 1. After splitting the images, the datasets corresponding to images of sizes 250 x 250, 500 x 500, and 1000 x 1000 pixels were comprised of 1804, 1112, and 570 images, respectively. Furthermore, the images were manually labelled as diseased, healthy, or background, and organized into training and testing folders in order to train deep learning models.

Table 1. Dataset distribution for training deep learning models for identifying diseased regions using tile segmentation.

Class	Training Images	Testing Images
Diseased (250 x 250)	349	348
Healthy (250 x 250)	251	251
Background (250 x 250)	303	302
Diseased (500 x 500)	255	254
Healthy (500 x 500)	164	163
Background (500 x 500)	138	138
Diseased (500 x 500)	124	123
Healthy (500 x 500)	137	136
Background (500 x 500)	25	25
TOTAL	1746	1740

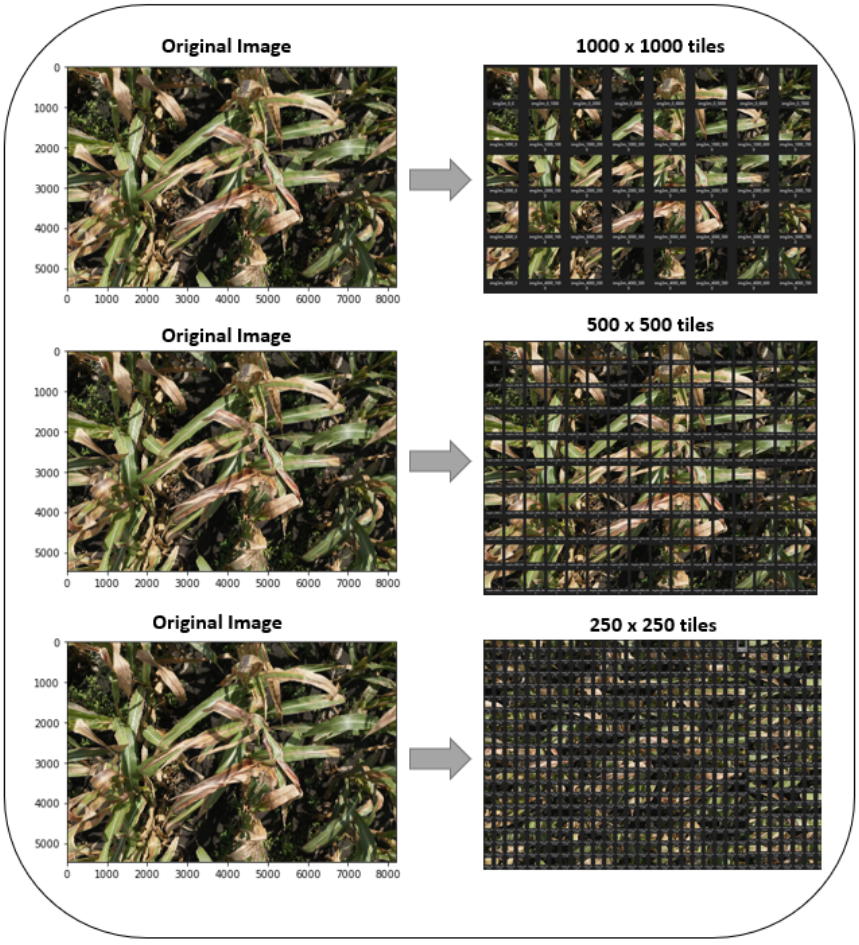

Fig 1. Overall Tile Dataset Generation Workflow.

SLIC Segmentiation

Superpixels are segments of an image that are created by grouping together different pixels within an image into perceptually meaningful atomic regions that may be similar in color, texture, and shape (Martins et al., 2021). Although different algorithms exist for creating superpixels, Simple Linear Iterative Clustering (SLIC) segmentation is a popular and a computationally efficient method to segment an image into multiple superpixels (Achanta et al., 2010).

When creating superpixels, the SLIC algorithms relies on two primary parameters, i.e., the number of segments that need to be created (K) and the compactness (m). The compactness determines the compactness of the pixels corresponding to superpixels. Essentially, by increasing the compactness (m), the compactness increases, and more regular quadrilateral contours are generated. However, by reducing the compactness (m), the superpixels are more irregular and it was observed to be better for differentiating between diseased and healthy regions within UAS acquired corn field imagery. After comparing different compactness (m) values, a single value was fixed for conducting the experiments in this study in order to maintain consistency. Therefore, the number of segments (K) was varied for testing the impact of changing the number of superpixels that were created per image. The number of segments (K) was also the only parameter that was modified in a recent study (Martins et al., 2021).

For SLIC segmentation in this study, superpixels were created using different combinations of parameters. For the images acquired at 3m, the compactness (m) value was 5 and 50 segments were created. In addition, for images acquired at 12m, the compactness (m) value was 5 and 100 segments were created. Finally, for images acquired at 20m, the compactness (m) value of 10 was used and 100 segments were created. This was done after testing with various compactness (m) values and number of segments.

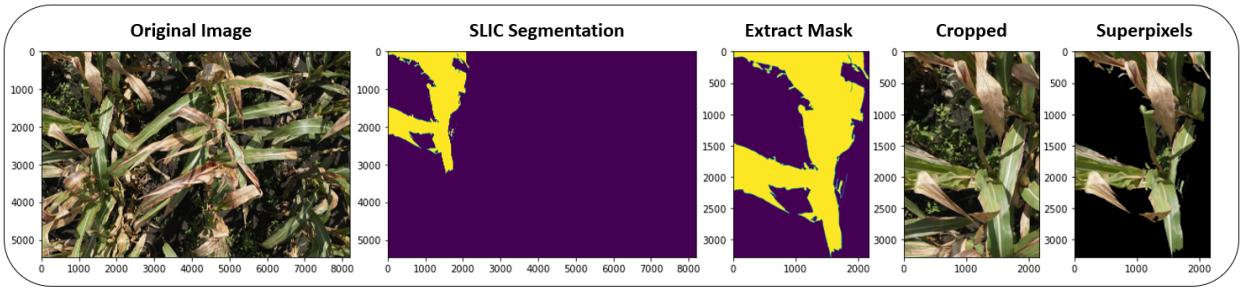

Fig 2. Overall SLIC Segmentation and Superpixels Dataset Generation Workflow.

Table 2. Dataset distribution for training deep learning models for identifying diseased regions using SLIC segmentation.

Class	Training Images	Testing Images
Diseased (m = 10)	121	121
Healthy (m = 10)	121	120
Background (m = 10)	121	121
Diseased (m = 5)	137	135
Healthy (m = 5)	136	136
Background (m = 5)	161	160
TOTAL	797	793

Deep Learning

Deep learning is a machine learning technique that relies on the use of deep neural networks (DNN) that are capable of accurately learning important features from training data for identification purposes.

A DNN typically consists of input layers, hidden layers, and an output layer. The input layer takes in the input images as tensors in a specified size as per the requirements of the deep learning DNN architecture. Multiple hidden layers follow the input layer. Hidden layers are comprised of convolutional layers, dense layers, pooling layers, or batch normalization layers. In addition, fully connected layers are then present followed by an output layer. The output layer consists of neurons corresponding to the total number of classes that being identified using either the Sigmoid activation function for a binary classification problem or the Softmax activation function for a multiclass classification problem.

Image classification is a deep learning technique where a probability is assigned to an image which corresponds to different classes that were used for training the model. Unlike object detection and semantic segmentation, traditional image classification is unable to accurate locate the identified objects using bounding boxes or masks. However, in this study image classification was used accurately locate and identify diseased regions within UAS imagery acquired in diseased corn fields by accurately identifying each tile or SLIC segment within an image.

Training robust deep learning-based image classification requires access to large imagery datasets consisting of thousands of images. One of the most popular datasets, ImageNet, is comprised of a total of 14 million images. Due to the availability of limited resources, access to such large datasets for disease identification is limited. Therefore, for the purpose of this study, transfer learning was used for training each model.

Transfer learning is a technique that is commonly used to train deep learning models when access to large datasets and computational resources is limited. Transfer learning helps training deep learning models by utilizing pre-trained weights from models that were trained for similar but different tasks. For image classification, the pre-trained ImageNet weights are most commonly used.

A total of five different state-of-the-art DNN architectures: namely VGG16 (Simonyan & Zisserman, 2014), ResNet50 (He et al., 2016), InceptionV3 (Szegedy et al., 2016), DenseNet169 (Huang et al., 2017), and Xception (Chollet, 2017), were utilized for the interest of this study. Transfer learning was used by utilizing pre-trained ImageNet weights for training deep learning models capable of locating diseased regions in corn fields from UAS imagery.

A total of 25 deep learning models were trained for the purpose of this study using the datasets that were created using the tile segmentation and SLIC segmentation approaches. Five models, using each of the DNN architectures, were trained for the tile segmentations that were created using tile sizes of 250 x 250, 500 x 500, and 1000 x 1000 pixels. The same five DNN architectures where then used to train the superpixels datasets that were created using compactness (m) of 5 and 10. Before training the models, the data augmentation techniques were used. Each image was augmented using the built-in TensorFlow functions by rotating, flipping, and zooming the images. In addition, each image was converted into tensors of input size corresponding to the input image size requirements for each DNN architecture. For VGG16, ResNet50, DenseNet169, and Xception, the training images were resized to 224 x 224 pixels. The input image size for InceptionV3 was 299 x 299 pixels. Each model was trained for a total of 25 epochs with a learning rate of 0.0001, the ADAM optimizer, and a batch size of 32 The categorical cross entropy loss function was also used. After training all the models, different metrics were used for evaluating and comparing their performances.

Evaluation Metrics

In order to evaluate the trained deep learning models, two primary evaluation metrics were utilized: namely confusion matrices and testing accuracies. In addition, the inference times were compared for the sliding window disease region location task.

$$testing\ accuracy = \frac{TP+FN}{TP+FP+TN+FP} \quad (1)$$

where TP = true positive, FP = false positive, TN = true negative, FN = false negative

Web and Smartphone Application Tool for Disease Region Identification

After training and comparing the deep learning models for accurately locating and identifying diseased regions within corn fields from UAS imagery, a disease regions identification tool was developed in the form of web and smartphone applications. The “Streamlit” Python library was used for creating the application. Streamlit is a library that helps easily deploy deep learning models for various tasks. In addition, Streamlit offers multiple additional promising tools to help users easy upload images for analysis.

The home page was developed to provide a user with the options of either using tile segmentation or SLIC segmentation for identifying the different diseased regions. The title of application is displayed at the top of the home page and a map that corresponds to the corresponding farm at which the data was collected.

After the user is prompted to select the type of segmentation approach for identifying the diseased regions, the user was prompted to upload an image. The uploaded image was then fed into a sliding window algorithm that iterates over each of the segments and classifies them as either diseased, healthy, or background using the trained deep learning model. If the region was identified as diseased, it was highlighted orange.

Using the “Exif” library from Python, the name of the image, the time at which the image was acquired, and the RTK geolocation coordinates at which the image was acquired were extracted. The area of the image that was diseased and the Exif information obtained from the image were then sent to the farmer via email communication. The “smtplib” library from Python for setting up an SMTP server was used to send email notifications. For the purpose of this study, a temporary Gmail account named farmerhack1@gmail.com was created to send emails with information corresponding to diseased regions identified from UAS imagery acquired in corn fields.

Resources

For the purpose of this study, the code was primarily written using the Python programming language. The TensorFlow 2.0 deep learning framework was utilized in order to train the deep learning models. Each model was trained using an NVIDIA RTX 3090 GPU. In addition, the

Python was used to develop the web application using an Apple MacBook Pro with Apple Silicon M1 Pro chip with 16 GPU cores and 10 CPU cores.

Results and Discussion

Tile Based Segmentation

For the first set of experiments, the dataset that was created by splitting the UAS images into tiles of size 250 x 250, 500 x 500, and 1000 x 1000 pixels, was used. For each of the three different tile sizes, five different deep learning-based image classification were trained for a total of 25 epochs using each of the five state-of-the-art DNN architectures: namely VGG16, ResNet50, InceptionV3, DenseNet169, and Xception.

Tile Size of 250 x 250 Pixels

The first set of models were trained using the tile segments of size 250 x 250 pixels. After the models were trained, the training and validation accuracy and loss plots were created. It was observed that apart from the ResNet50 model that did not seem to train, the validation accuracy for the other models reached up to 100%. In addition, it was observed from the plots that the VGG16 had a higher degree of overfitting and the validation accuracy for the inception model started to decrease towards the end of training which indicates some degree of overfitting. Nevertheless, it is important to evaluate the modes by comparing the testing accuracies.

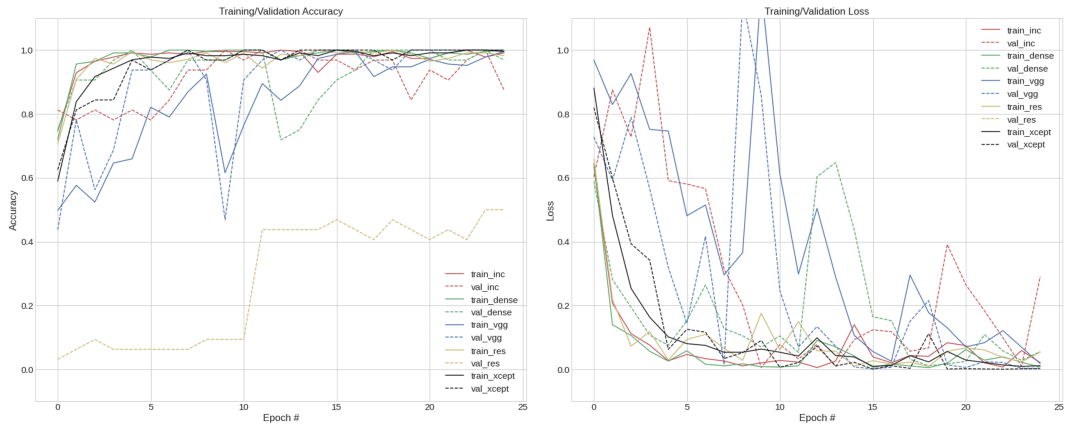

Fig 3. Training and validation accuracy and loss plots for training deep learning models to identifying diseased regions using tile segments of size 250 x 250 pixels.

In addition, the testing accuracies and testing losses were also obtained using the testing dataset, as shown in table 3 below. It was observed that 100% testing accuracy was achieved for the VGG16, DenseNet160, and Xception models. The lowest testing loss was achieved for the Xception model. Therefore, when tile size of 250 x 250 pixels was used, the Xception model performed the best.

Table 3. Testing accuracies and testing loss when tile size of 250 x 250 pixels was used.

Model	Testing Accuracy	Testing Loss
InceptionV3	93.75%	0.1242
ResNet50	56.25%	15.0615
VGG16	100%	0.0041
DenseNet169	100%	0.0251
Xception	100%	0.0007

Tile Size of 500 x 500 Pixels

Once again, five models were trained for identifying diseased regions within the UAS imagery of diseased corn fields using the tiles of size 500 x 500 pixels that were created. First, the training and validation accuracies and losses were plotted. In addition, almost no overfitting was observed as there were very small fluctuations in the plots that were generated. The ResNet50 model again failed to train, and validation accuracy did not cross 50%.

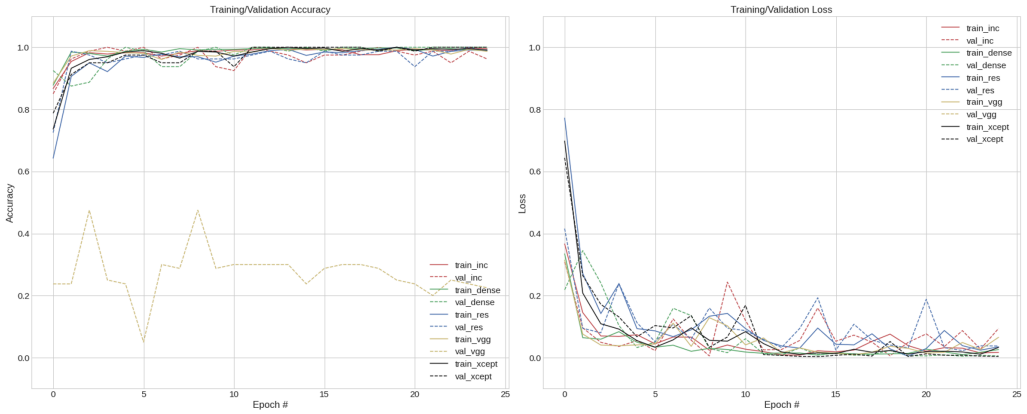

Fig 4. Training and validation accuracy and loss plots for training deep learning models to identifying diseased regions using tile segments of size 500 x 500 pixels.

After the plots were generated, the testing accuracies and testing losses were obtained and compared. The testing accuracies was 100% for InceptionV3, VGG16, DenseNet169 and Xception. After evaluating the testing losses, it was observed that the InceptionV3 achieved the best performance as it had the lowest testing loss of 0.0045. The results are shown in table 4.

Table 4. Testing accuracies and testing loss when tile size of 500 x 500 pixels was used.

Model	Testing Accuracy	Testing Loss
InceptionV3	100%	0.0045
ResNet50	25.00%	8.3028
VGG16	100%	0.0077
DenseNet169	100%	0.0048
Xception	100%	0.0265

Tile Size of 1000 x 1000 Pixels

Finally, tile segments of size 1000 x 1000 pixels were used for training the models. Once again, a low degree of overfitting was observed as almost no fluctuation existing in the training and validation accuracy and loss plots as shown in figure 5. In the case of larger tile sizes, the testing accuracy for ResNet50 improved.

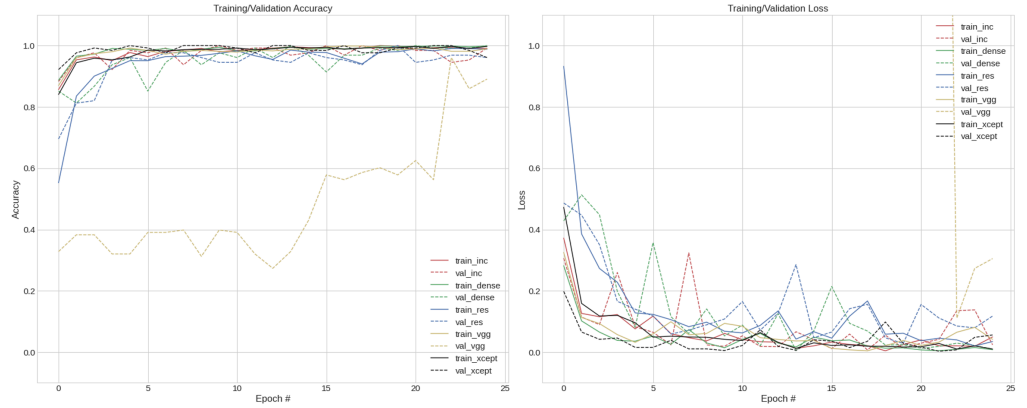

Fig 5. Training and validation accuracy and loss plots for training deep learning models to identifying diseased regions using tile segments of size 1000 x 1000 pixels.

Testing accuracies and testing losses were once again compared for evaluating the overall performance of the models. The testing accuracies for InceptionV3, VGG16, DenseNet169 and Xception were 100%. Unlike ResNet50 models that were trained for tile segments of sizes 250 x 250 pixels and 500 x 500 pixels, the testing accuracy was high at 87.5% when tile segments were 1000 x 1000 pixels. The best model, however, was the DenseNet160 model as it achieved the highest testing accuracy of 100% and the lowest testing loss of 0.0003.

Table 5. Testing accuracies and testing loss when tile size of 1000 x 1000 pixels was used.

Model	Testing Accuracy	Testing Loss
InceptionV3	100%	0.0242
ResNet50	87.5%	0.3000

VGG16	100%	0.0190
DenseNet169	100%	0.0003
Xception	100%	0.0023

SLIC Segmentation

For the second set of experiments, the dataset that was created by splitting the UAS images into superpixels using SLIC segmentation, was used. Two different compactness (m) values were used, i.e., 5 and 10.

Superpixels Created Using Compactness (m) of 5

When the compactness (m) value was set to 5, the superpixels that were created consisted of more irregular boundaries. After the dataset was prepared with diseased, healthy, and background superpixels, the five DNN architectures were used to train five different models. After training, the training and validation accuracy and loss plots were created as shown in figure 6. It was observed that there was a larger degree of overfitting as the validation loss values fluctuated throughout training. The ResNet50 model again failed to train well, and validation accuracy did not cross 50%.

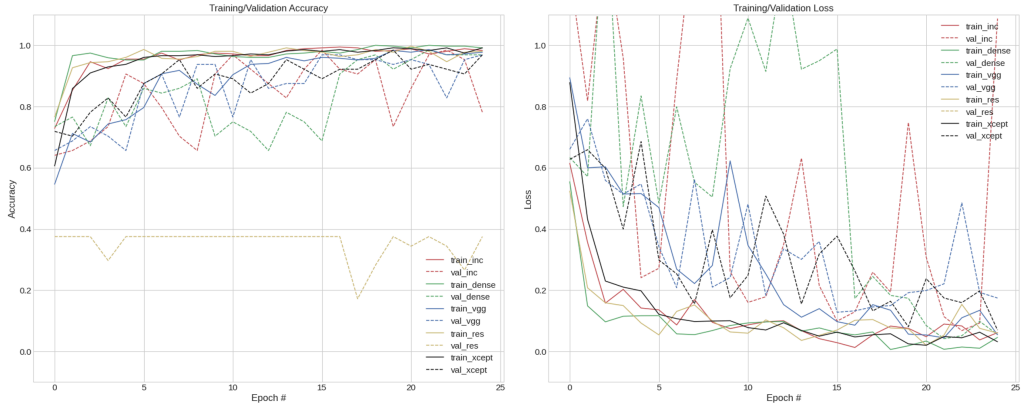

Fig 6. Training and validation accuracy and loss plots for training deep learning models to identifying diseased regions using SLIC segments with compactness (m) value of 5.

In addition, the testing accuracies and testing losses were also obtained using the testing dataset, as shown in table 6. The highest testing accuracy of 93.75% was achieved for the VGG16 model and the corresponding testing loss was 0.01872. No other model achieved testing accuracies of greater than 90%.

Table 7. Use the Table Caption style above each table. Material in the table uses the Table Contents style. Use standard Word table commands or make a table in your usual way.

Model	Testing Accuracy	Testing Loss
InceptionV3	81.25%	0.9234
ResNet50	25.00%	5.4016
VGG16	93.75%	0.1872
DenseNet169	81.25%	0.2556
Xception	81.25%	0.4240

Superpixels Created Using Compactness (m) of 10

In order to conduct further experiments, the superpixels that were created using compactness (m) value of 10 was used. The training and validation accuracy and loss plots were created and are shown in figure 7. With a higher compactness (m) value, the validation accuracy and loss values did not closely follow the training accuracy and loss which is representative of a higher degree of overfitting.

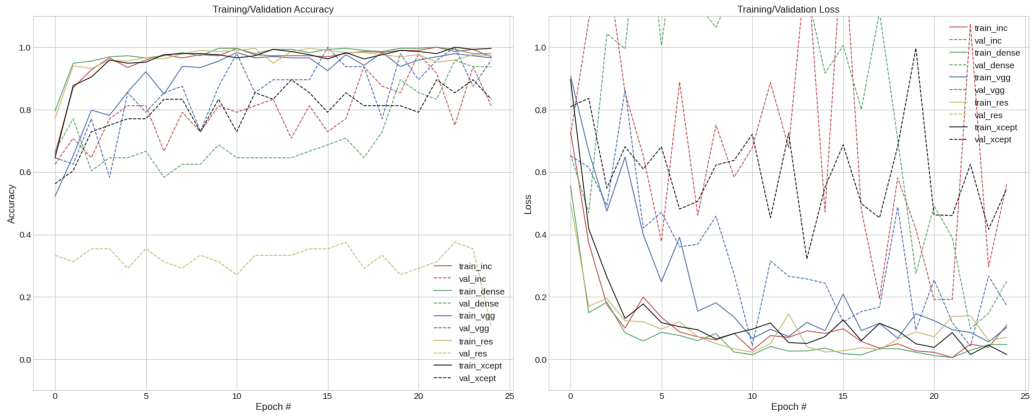

Fig 6. Training and validation accuracy and loss plots for training deep learning models to identifying diseased regions using SLIC segments with compactness (m) value of 10.

However, in order to further assess the performance of the models, the testing accuracies and losses were compared. It was observed that the DenseNet169 model achieved the highest testing accuracy and lowest testing loss of 93.75% and 0.2469 respectively.

Table 6. Use the Table Caption style above each table. Material in the table uses the Table Contents style. Use standard Word table commands or make a table in your usual way.

Model	Testing Accuracy	Testing Loss
InceptionV3	87.5%	0.5060
ResNet50	6.25%	3.613
VGG16	81.25%	0.3636
DenseNet169	93.75%	0.2469
Xception	75.00%	0.6832

Sliding Window Disease Reigon Identification

After comparing the performances of the different segmentation types, it was observed that the tile segmentation yielded higher overall results for accurately identifying the diseased regions present within corn fields. The testing accuracies using tile segmented reached up to 100%, whereas for SLIC segmentation, the highest testing accuracy was 93.75%. Therefore, the tile segmentation algorithm that was trained to identifying the tiles of size 1000 x 1000 pixels was first used to identify and highlight the diseased regions. The sliding window was used over the image. If the regions were diseased, it was highlighted orange as shown in figure 8. In addition, the area of diseased region was calculated with respect to the area of the entire image, and it was reported in the title of the image.

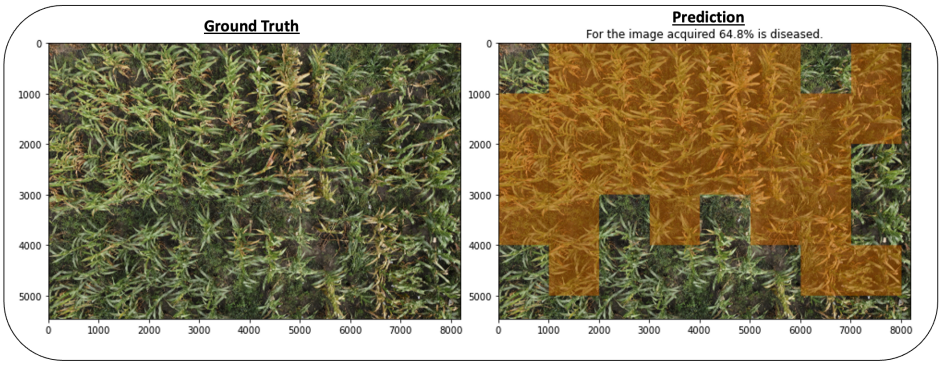

Fig 8. Sliding window algorithm to identify and highlight diseased regions in UAS imagery acquired in diseased fields.

Web and Smartphone Applications

After training the deep learning models capable of accurately locating the different diseased regions present within corn fields using two different segmentation approaches, and after developing the sliding window algorithm for highlighting the diseased regions, a web application was developed using the Streamlit API.

The home page of the application displays the title and consists of the map with a pinpoint on where the farms or fields where data was collected are located. In addition, the drop-down box on the top left of the screen prompts the user to select the type of different segmentation algorithms to choose as shown in figure 9. If the user selected the tile segmentation algorithm as shown in figure 9, the best model that achieved the highest testing accuracy was used for identifying the diseased regions.

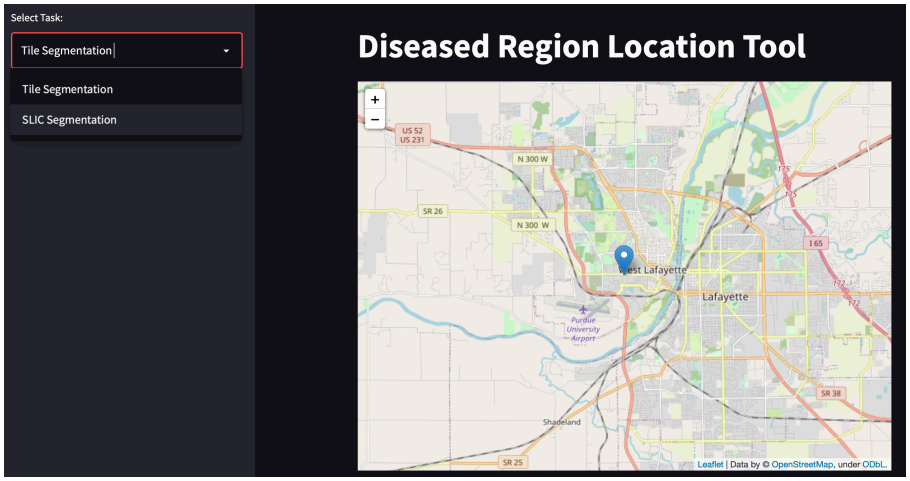

Fig 9. Home page of the Disease Region Location Tool web application.

After the user chooses the option that they would like to use for identifying the different diseased regions within corn fields, the user is prompted to upload an image as shown in figure 10. The image can be selected from the computer.

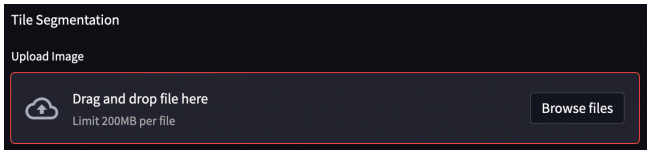

Fig 10. Image upload box.

Once the image is uploaded, the Pillow library in python is used for reading the information and the segmentation is performed. If the tile segmentation was selected, the original images were split into sizes of 1000 x 1000 pixels. Each of the tiles were then passed into the trained deep learning model and were identified as either diseased, healthy, or soil. All the regions that were diseased were highlighted orange to indicate the diseased parts of the image corresponding to a region in the field as shown in figure 11. In addition, the percentage of the image which consists of diseased regions was calculated and the information was displayed for the user.

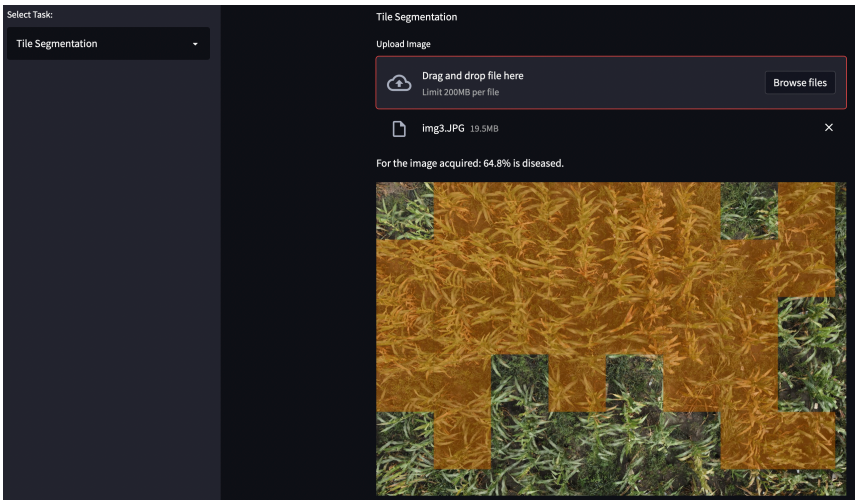

Fig 11. Identification of diseased regions in corn fields using the Disease Region Location Tool web application.

Finally, the geolocation information corresponding to each image that was obtained from the RTK base station was used to locate the image on the map (figure 12). The total area corresponding to the diseased regions, the name of the image, the date and time of image acquisition, and the coordinates were then sent to the user in the form of an email. This link could be either opened using the smartphone or a web application in order to help update farmers on diseased information for their fields.

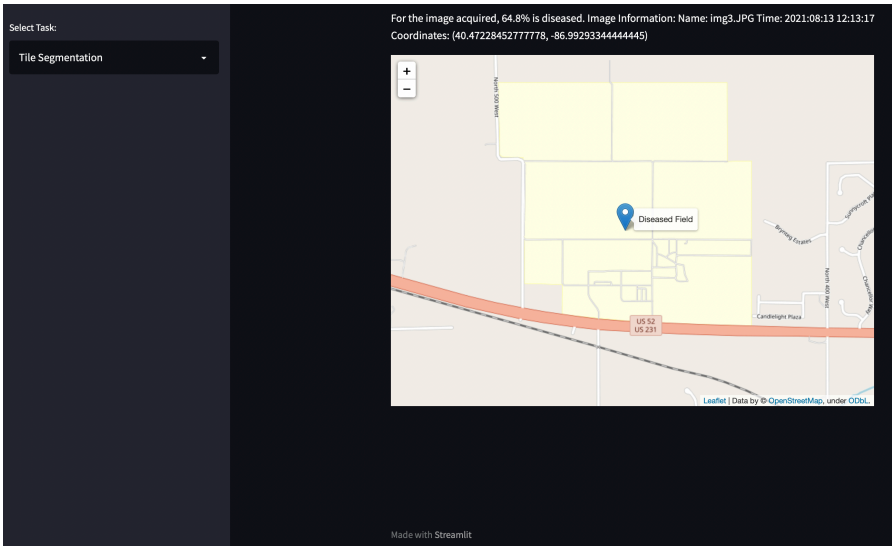

Fig 12. Pinpoint diseased regions on maps using RTK geolocation information.

Once the email was sent, the notification was then displayed in the notifications of a smartphone. A sample of the email that was sent / received is shown in figure 13. The information can help farmers keep track of disease information in different parts of their fields over a period of time.

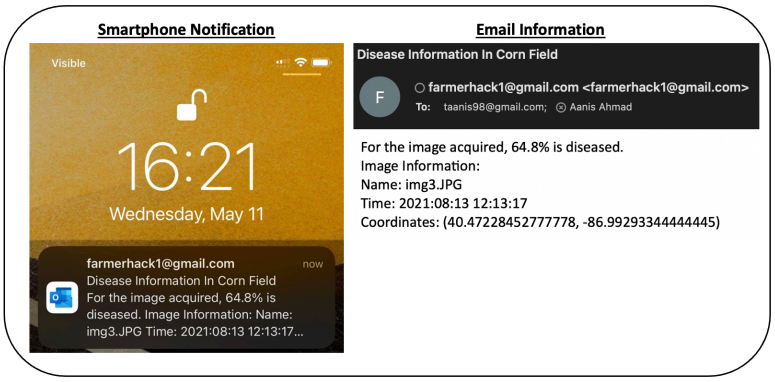

Fig 13. Email notification corresponding to diseased corn fields sent to farmers from the Disease Region Location Tool.

Although using a web application is useful, many farmers are also likely to use the application in fields in real-time. Therefore, the application can also be used from a smartphone as shown in figure 14. The task can be selected, and the original location is shown on the home page. When uploading the image for analysis and disease diagnosis, the images can be uploaded from the gallery. In addition, the smartphone application provides the benefit of taking an image on the go. After the image is uploaded, once again the disease regions are identified, and a map is displayed with the information for the diseased corn field. Finally, the information is also sent to the farmer in the form of an email.

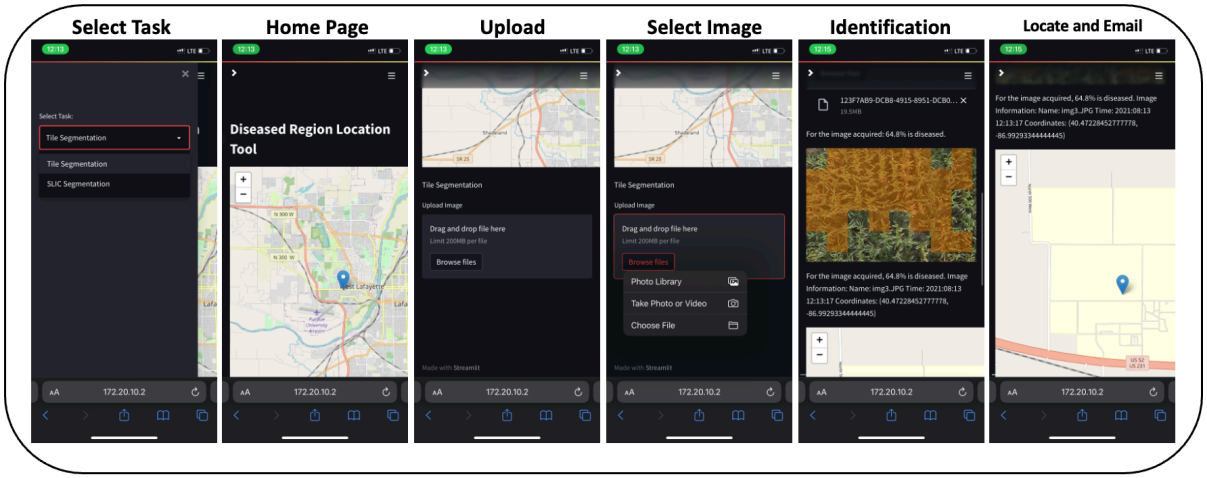

Fig 14. Disease Region Location Tool smartphone application.

Conclusion

In this study, a deep learning-based disease region identification tool was developed in the form of web and smartphone applications. Two different segmentation techniques: namely tile and SLIC segmentation were used to create tiles of varying sizes and superpixels with different compactness (m) values. Tiles of sizes 250 x 250, 500 x 500, and 1000 x 1000 pixels were created and labelled as either diseased, healthy, or background. In addition, SLIC segmentation was used to create superpixels with compactness (m) values of 5 and 10. The datasets that were created using each of the three tile sizes and two compactness (m) values were then used to train deep learning models using five different DNN architectures: namely VGG16, ResNet50, InceptionV3, DenseNet169, and Xception. It was observed that the tile segmentation achieved high testing accuracies of up to 100% for each of the tile sizes. However, for the superpixels that were created using SLIC segmentation, testing accuracies of up to 93.75% were achieved. Furthermore, the best performing model was the DenseNet169 model that was trained to identifying diseased regions in corn fields when images were segmented into tiles of sizes 1000 x 1000 pixels resulting in a testing accuracy of 100% and testing loss of 0.0007. A sliding window algorithm was then used to highlight diseased regions from UAS acquired imagery in diseased corn fields. The trained models were then deployed onto a web and smartphone application in order to help farmers identifying diseased regions in corn fields. Additionally, RTK geolocation information from each image was extracted and sent to the farmers to indicate the location of diseased regions. Finally, after analyzing uploaded images corresponding to diseased regions within corn fields, the information was sent via email communication to update farmers in real-time. Overall, in this study, a deep learning-based tool was developed to help farmers analyze diseased corn fields using UAS imagery.

Future works include enhancing the application that was created by adding multiple additional features. In particular, a link to the map will be sent to the farmer along with a link to the application via email communication. In addition, a map will be created highlighting the entire field and corresponding diseased regions in order to provide the information regarding the area of the field that is diseased on different dates.

Acknowledgements

The research was made possible by the funding provided by Wabash Heartland Innovation Network (WHIN) grant number 18024589 and the USDA National Institute of Food and Agriculture (NIFA) Hatch project 1012501.

References

Achanta, R., Shaji, A., Smith, K., Lucchi, A., Fua, P., & Süsstrunk, S. (2010). Slic superpixels (No. REP_WORK).

Achanta, R., Shaji, A., Smith, K., Lucchi, A., Fua, P., & Süsstrunk, S. (2012). SLIC superpixels compared to state-of-the-art superpixel methods. IEEE transactions on pattern analysis and machine intelligence, 34(11), 2274-2282.

Ahmad, A., Saraswat, D., Aggarwal, V., Etienne, A., & Hancock, B. (2021a). Performance of deep learning models for classifying and detecting common weeds in corn and soybean production systems. Computers and Electronics in Agriculture, 184, 106081.

Ahmad, A., Saraswat, D., El Gamal, A., & Johal, G. S. (2021b). Comparison of deep learning models for corn disease identification, tracking, and severity estimation using images acquired from uav-mounted and handheld sensors. In 2021 ASABE Annual International Virtual Meeting (p. 1). American Society of Agricultural and Biological Engineers.

Bock, C. H., Poole, G. H., Parker, P. E., & Gottwald, T. R. (2010). Plant disease severity estimated visually, by digital photography and image analysis, and by hyperspectral imaging. Critical reviews in plant sciences, 29(2), 59-107.

Chen, J., Zhang, D., Zeb, A., & Nanehkaran, Y. A. (2021). Identification of rice plant diseases using lightweight attention networks. Expert Systems with Applications, 169, 114514.

Chollet, F. (2017). Xception: Deep learning with depthwise separable convolutions. In Proceedings of the IEEE conference on computer vision and pattern recognition (pp. 1251-1258).

Etienne, A., Ahmad, A., Aggarwal, V., & Saraswat, D. (2021). Deep Learning-Based Object Detection System for Identifying Weeds Using UAS Imagery. Remote Sensing, 13(24), 5182.

Farber, C., Mahnke, M., Sanchez, L., & Kurouski, D. (2019). Advanced spectroscopic techniques for plant disease diagnostics. A review. TrAC Trends in Analytical Chemistry, 118, 43-49.

Huang, G., Liu, Z., Van Der Maaten, L., & Weinberger, K. Q. (2017). Densely connected convolutional networks. In Proceedings of the IEEE conference on computer vision and pattern recognition (pp. 4700-4708).

He, K., Zhang, X., Ren, S., & Sun, J. (2016). Deep residual learning for image recognition. In Proceedings of the IEEE conference on computer vision and pattern recognition (pp. 770-778).

Jahan, N., Zhang, Z., Liu, Z., Friskop, A., Flores, P., Mathew, J. J., & Das, A. K. (2021). Using images from a handheld camera to detect wheat bacterial leaf streak disease severities. In 2021 ASABE Annual International Virtual Meeting (p. 1). American Society of Agricultural and Biological Engineers.

Kerkech, M., Hafiane, A., & Canals, R. (2020). Vine disease detection in UAV multispectral images using optimized image registration and deep learning segmentation approach. Computers and Electronics in Agriculture, 174, 105446.

Kitano, B. T., Mendes, C. C., Geus, A. R., Oliveira, H. C., & Souza, J. R. (2019). Corn plant counting using deep learning and UAV images. IEEE Geoscience and Remote Sensing Letters.

Martins, J. A. C., Menezes, G., Gonçalves, W., Sant'Ana, D. A., Osco, L. P., Liesenberg, V., ... & Junior, J. M. (2021). Machine learning and SLIC for Tree Canopies segmentation in urban areas. Ecological Informatics, 66, 101465.

Ngugi, L. C., Abelwahab, M., & Abo-Zahhad, M. (2021). Recent advances in image processing techniques for automated leaf pest and disease recognition–A review. Information processing in agriculture, 8(1), 27-51.

Nguyen, C., Sagan, V., Maimaitiyiming, M., Maimaitijiang, M., Bhadra, S., & Kwasniewski, M. T. (2021). Early detection of plant viral disease using hyperspectral imaging and deep learning. Sensors, 21(3), 742.

Simonyan, K., & Zisserman, A. (2014). Very deep convolutional networks for large-scale image recognition. arXiv preprint arXiv:1409.1556.

Szegedy, C., Vanhoucke, V., Ioffe, S., Shlens, J., & Wojna, Z. (2016). Rethinking the inception architecture for computer vision. In Proceedings of the IEEE conference on computer vision and pattern

recognition (pp. 2818-2826).

Tetila, E. C., Machado, B. B., Menezes, G. V., de Souza Belete, N. A., Astolfi, G., & Pistori, H. (2019a). A deep-learning approach for automatic counting of soybean insect pests. IEEE Geoscience and Remote Sensing Letters, 17(10), 1837-1841.

Tetila, E. C., Machado, B. B., Menezes, G. K., Oliveira, A. D. S., Alvarez, M., Amorim, W. P., ... & Pistori, H. (2019b). Automatic recognition of soybean leaf diseases using UAV images and deep convolutional neural networks. IEEE geoscience and remote sensing letters, 17(5), 903-907.

Thenmozhi, K., & Reddy, U. S. (2019). Crop pest classification based on deep convolutional neural network and transfer learning. Computers and Electronics in Agriculture, 164, 104906.

Trindade, L. D. G., Basso, F. P., Macedo Rodrigues, E. D., Bernardino, M., Welfer, D., & Müller, D. (2020, December). Analysis of the Superpixel Slic Algorithm for Increasing Data for Disease Detection Using Deep Learning. In International Conference on Intelligent Systems Design and Applications (pp. 488-497). Springer, Cham.

Tudi, M., Daniel Ruan, H., Wang, L., Lyu, J., Sadler, R., Connell, D., ... & Phung, D. T. (2021). Agriculture development, pesticide application and its impact on the environment. International journal of environmental research and public health, 18(3), 1112.

Wang, A. X., Tran, C., Desai, N., Lobell, D., & Ermon, S. (2018, June). Deep transfer learning for crop yield prediction with remote sensing data. In Proceedings of the 1st ACM SIGCAS Conference on Computing and Sustainable Societies(pp. 1-5).

Wang, C., Du, P., Wu, H., Li, J., Zhao, C., & Zhu, H. (2021). A cucumber leaf disease severity classification method based on the fusion of DeepLabV3+ and U-Net. Computers and Electronics in Agriculture, 189, 106373.

Wiesner-Hanks, T., Stewart, E. L., Kaczmar, N., DeChant, C., Wu, H., Nelson, R. J., ... & Gore, M. A. (2018). Image set for deep learning: field images of maize annotated with disease symptoms. BMC research notes, 11(1), 1-3.

Wu, H., Wiesner-Hanks, T., Stewart, E. L., DeChant, C., Kaczmar, N., Gore, M. A., ... & Lipson, H. (2019). Autonomous detection of plant disease symptoms directly from aerial imagery. The Plant Phenome Journal, 2(1), 1-9.

Xie, Q., Wang, J., Lopez-Sanchez, J. M., Peng, X., Liao, C., Shang, J., ... & Ballester-Berman, J. D. (2021). Crop height estimation of corn from multi-year RADARSAT-2 polarimetric observables using machine learning. Remote Sensing, 13(3), 392.

Young, S. N., Kayacan, E., & Peschel, J. M. (2019). Design and field evaluation of a ground robot for high-throughput phenotyping of energy sorghum. Precision Agriculture, 20(4), 697-722.

Zhu, H., Chu, B., Zhang, C., Liu, F., Jiang, L., & He, Y. (2017). Hyperspectral imaging for presymptomatic detection of tobacco disease with successive projections algorithm and machine-learning classifiers. Scientific Reports, 7(1), 1-12.